

Journal of Materials Chemistry C

Accepted Manuscript



This is an *Accepted Manuscript*, which has been through the Royal Society of Chemistry peer review process and has been accepted for publication.

Accepted Manuscripts are published online shortly after acceptance, before technical editing, formatting and proof reading. Using this free service, authors can make their results available to the community, in citable form, before we publish the edited article. We will replace this *Accepted Manuscript* with the edited and formatted *Advance Article* as soon as it is available.

You can find more information about *Accepted Manuscripts* in the [Information for Authors](#).

Please note that technical editing may introduce minor changes to the text and/or graphics, which may alter content. The journal's standard [Terms & Conditions](#) and the [Ethical guidelines](#) still apply. In no event shall the Royal Society of Chemistry be held responsible for any errors or omissions in this *Accepted Manuscript* or any consequences arising from the use of any information it contains.

Molecular design for a cybotactic nematic phase

Wataru Nishiya,^a Yoichi Takanishi,^b Jun Yamamoto^b and Atsushi Yoshizawa^{*, a}

^aDepartment of Frontier Materials Chemistry, Graduate School of Science and Technology, Hirosaki University, 3 Bunkyo-cho, Hirosaki, Aomori 036-8561, Japan

E-mail: ayoshiza@cc.hirosaki-u.ac.jp

^bDepartment of Physics, Graduate School of Science, Kyoto University, Oiwake-cho, Kitashirakawa, Sakyo-ku, Kyoto, 606-8562, Japan

Abstract

Cybotactic nematic phase (Ncyb) has attracted much attention, however, almost all molecules under investigation have had a bent-shaped structure. We designed a U-shaped compound and some rod-like compounds possessing a terminal hydroxyl group. Then we investigated their phase transition behaviour using polarized optical microscopy, differential scanning calorimetry, and X-ray diffraction. The U-shaped compound possessing two 1,4-diphenyl-2,3-difluorobenzene units was found to exhibit an Ncyb phase with a temperature range of 20 K and an smectic C (SmC) phase. The layer spacing in these phases decreases continuously with decreasing temperature. The rod-like compound, 4-[4-(6-hydroxyhexyloxy)phenyl]-1-(4-hexyloxyphenyl)-2,3-difluorobenzene, was found to exhibit an Ncyb with a temperature range of 25 K and an SmC phase. The layer spacing shows discontinuous decrease at the Ncyb–SmC transition. This report presents two approaches for producing an Ncyb phase, i.e., (1) the introduction of the lateral correlation in the U-shaped compounds and (2) the introduction of the different terminal groups in the rod-shaped compounds.

Introduction

Nematic liquid crystals are described as differing from normal isotropic liquids only in the spontaneous orientation of the molecules with their long axes parallel. However, nematics of different types have been reported. De Vries presented the existence of more than one type of nematic based on the observation of four off-meridional X-ray scattering peaks.^{1,2} The short-range structure in nematics using X-ray diffraction was also reported by Chystyakov and Chailkowsky.³ Nematic phase with smectic-like ordering is ascribed to transient, local, and positional order in the nematic in the form of smectic fluctuations having the smectic layer either normal or tilted relative to nematic director \mathbf{n} (Fig. 1).⁴ Such a nematic phase, called cybotactic nematic, is denoted as Ncyb. Freiser predicted nematic of a new type having three directors termed as a biaxial nematic (Nb).⁵ The Nb phase was detected in a lyotropic liquid crystal⁶ and in side polymers.⁷ The Nb phase is expected to be of fundamental interest for general soft matter physics and for use in display applications with an order of magnitude faster expected switching times than the existing uniaxial nematics. According to theoretical predictions,^{9–10} numerous attempts have been undertaken,¹¹ such as with board-like molecules or by combining rod-like and disk-like units.^{12–14} However, an Nb phase was not confirmed in the systems. Bent-core mesogens, which are far away from the theoretically predicted structures, were reported to exhibit an Nb phase.^{15,16} However, controversy persists about the correct interpretation of the characteristics of the nematic phase formed by those bent-core molecules. Recently, Francescangeli and Samulski reported that the nematic phase of the bent-core mesogen (ODBP-Ph-O-C₄H₉) comprises inherently biaxial clusters of mesogens.¹⁷ It was proposed that local biaxiality can arise in the Ncyb phases composed of small clusters with smectic structure.^{18,19} Cybotactic clusters have been investigated intensively for consideration in the field of biaxial nematic liquid crystals.^{11,20} Detailed investigations on nematic phases of bent-core mesogens have been performed.²¹ Furthermore, bent-core molecules possessing a cybotactic structure in the N phase are reported to stabilize blue phases.^{22,23} Therefore, Ncyb phase has attracted much attention. Nevertheless, almost all molecules under investigation have had a bent-shaped structure.^{24–34} With respect to the formation of cybotactic clusters, they can be formed by intermolecular interactions even in liquids.²⁰ Supramolecular interactions such as dipole–dipole interactions and hydrogen bonding, which are strongly directional, can assist the formation of clusters in liquid crystalline phases.^{11,35}

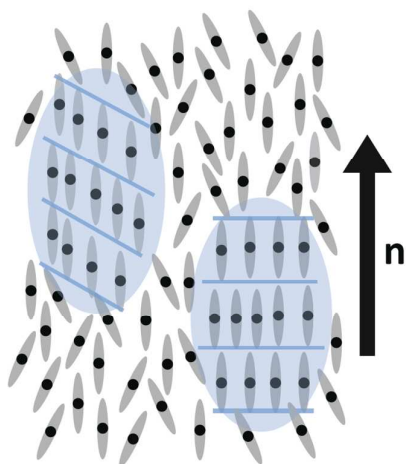


Fig. 1 Sketch of a nematic phase exhibiting skewed (left) and normal (right) smectic fluctuations.

Yoshizawa and Yamaguchi reported that a U-shaped compound exhibits a nematic phase possessing smectic-like layer structures and that the nematic phase presents the possibility of a phase biaxiality.³⁶ Later, a relation between cluster formation in a nematic phase and occurrence of the phase biaxiality was noted more clearly.³⁷ Not only the U-shaped system but also a hydrogen-bonding system can produce Ncyb phase. Recently, we reported a simple rod-like molecule possessing a terminal hydroxyl group, 4-[4-(7-hydroxyheptyloxy)phenyl]-1-(4-hexylphenyl)-2,3-difluorobenzene (*n*-hexyl derivative) exhibiting a nematic phase possessing cybotactic clusters and smectic C (SmC) phases consisting of three states:³⁸ conventional SmC with a monolayer structure, SmC' with a modulated bilayer structure possessing an in-plane modulation of molecular arrangement³⁹ and SmC'' with a bilayer structure. The structure–property relation in the rod-like compounds indicates that the phase transition behaviour is explainable in terms of competition between micro-segregation and anti-parallel molecular alignment in each layer.⁴⁰ Although the U-shaped compound and the rod-like compound showed Ncyb phases, the temperature ranges are insufficiently wide for investigation of temperature dependent properties. This report presents two approaches for producing an Ncyb phase, i.e., (1) the introduction of the lateral correlation in the U-shaped compounds and (2) the introduction of the different terminal groups in the rod-shaped compounds.

Experimental

Materials

Spectroscopic analysis. The purity of the final compound was confirmed using elemental analysis (EA 1110; CE Instruments Ltd.). Infrared (IR) spectroscopy (FTS-30; Bio-Rad Laboratories Inc.) and proton nuclear magnetic resonance (^1H NMR) spectroscopy (JNM-ECA500; JEOL) elucidated the structure of the final product.

Preparation of materials. For use in this study, 4-hydroxyphenyl-1-[4-(2-tetrahydropyranyloxy)phenyl]-2,3-difluorobenzene was purchased from Midori Kagaku Co. Ltd.

1,2-Bis{6-[4-(4-(4-hexyloxyphenyl)-2,3-difluorophenyl)phenoxy]hexyloxy}benzene (1). Compound **1** was prepared by a synthetic method as depicted in Scheme 1. Potassium carbonate (293 mg, 2.12 mmol) was added to a solution of 4-hydroxyphenyl-1-[4-(2-tetrahydropyranyloxy)phenyl]-2,3-difluorobenzene (500 mg, 1.31 mmol) and 1-bromohexane (110 mg, 0.66 mmol) in cyclohexanone (10 mL). The reaction mixture was stirred at 110 °C for 9 h. After filtration of the precipitate, the solvent was removed by evaporation. The residue was purified on silica gel using column chromatography with a dichloromethane and hexane (1:1) mixture as the eluent. It was then recrystallized from hexane, giving 4-hexyloxyphenyl-1-[4-(2-tetrahydropyranyloxy)phenyl]-2,3-difluorobenzene; yield 495 mg (81%); mp 108.5–109.2 °C.

Consequently, the obtained compound (490 mg, 1.05 mmol) was added to a solution of EtOH (20 mL) and 20% aq. HCL (4 mL). The resulting solution was stirred at 25 °C for 2 h. 40 mL of distilled water was added to the reaction mixture. The solution was extracted using dichloromethane (40 mL \times 3). The organic layers were combined, dried over magnesium sulphate, filtered, and evaporated to give 4-(4-hexyloxyphenyl)-1-(4-hydroxyphenyl)-2,3-difluorobenzene; yield 323 mg (80%); mp 182.1–183.5 °C.

Potassium carbonate (987 mg, 7.14 mmol) was added to a solution of 2-hydroxyphenol (513 mg, 4.66 mmol) and 1,6-dibromohexane (2.5 g, 10.2 mmol) in cyclohexanone (10 mL). The reaction mixture was stirred at 140 °C for 7 h. After filtration of the precipitate, the solvent was removed by evaporation. The residue was purified on silica gel using column chromatography with a toluene and ethyl acetate (4:1) mixture as the eluent, giving 1,2-bis(6-dibromohexyloxy)benzene as a colourless liquid; yield 600 mg (30%).

Potassium carbonate (82 mg, 0.59 mmol) was added to a solution of 4-(4-hexyloxyphenyl)-1-(4-hydroxyphenyl)-2,3-difluorobenzene (115 mg, 0.30 mmol) and 1,2-bis(6-dibromohexyloxy)benzene (230 mg, 0.53 mmol) in cyclohexanone (10 mL). The reaction mixture was stirred at 120 °C for 10 h. After filtration of the precipitate, the solvent was removed by evaporation. The residue was washed with EtOH and purified on silica gel using column chromatography with a toluene and hexane (4:1) mixture as the eluent. It was then washed with EtOH, giving the desired compound; yield 31 mg (20%); mp 131.5-131.9 °C.

¹H-NMR (500 MHz, CDCl₃, TMS) δ_H/ppm: 7.49 (dd, 8H, Ar-H, *J* = 8.6, 2.9 Hz), 6.98 (d, 4H, Ar-H, *J* = 6.3 Hz), 6.98 (d, 4H, Ar-H, *J* = 6.3 Hz), 6.96 (d, 4H, Ar-H, *J* = 6.3 Hz), 6.91 (s, 4H, Ar-H), 4.04–3.99 (m, 12H, -OCH₂-), 1.83–1.36 (m, 32H, aliphatic-H), 0.92(t, 6H, -CH₃, *J* = 6.9 Hz). IR(KBr) ν cm⁻¹: 3422, 1609, 1526, 1462, 1078, 812. Elemental analysis: Found: C% 74.59; H% 7.66, Calc. for C₃₀H₃₆O₃F₂: C% 74.66; H% 7.52.

The other compounds presented in this paper were obtained using a similar method to that for compound **1**. Analytical data for the other compounds are listed below.

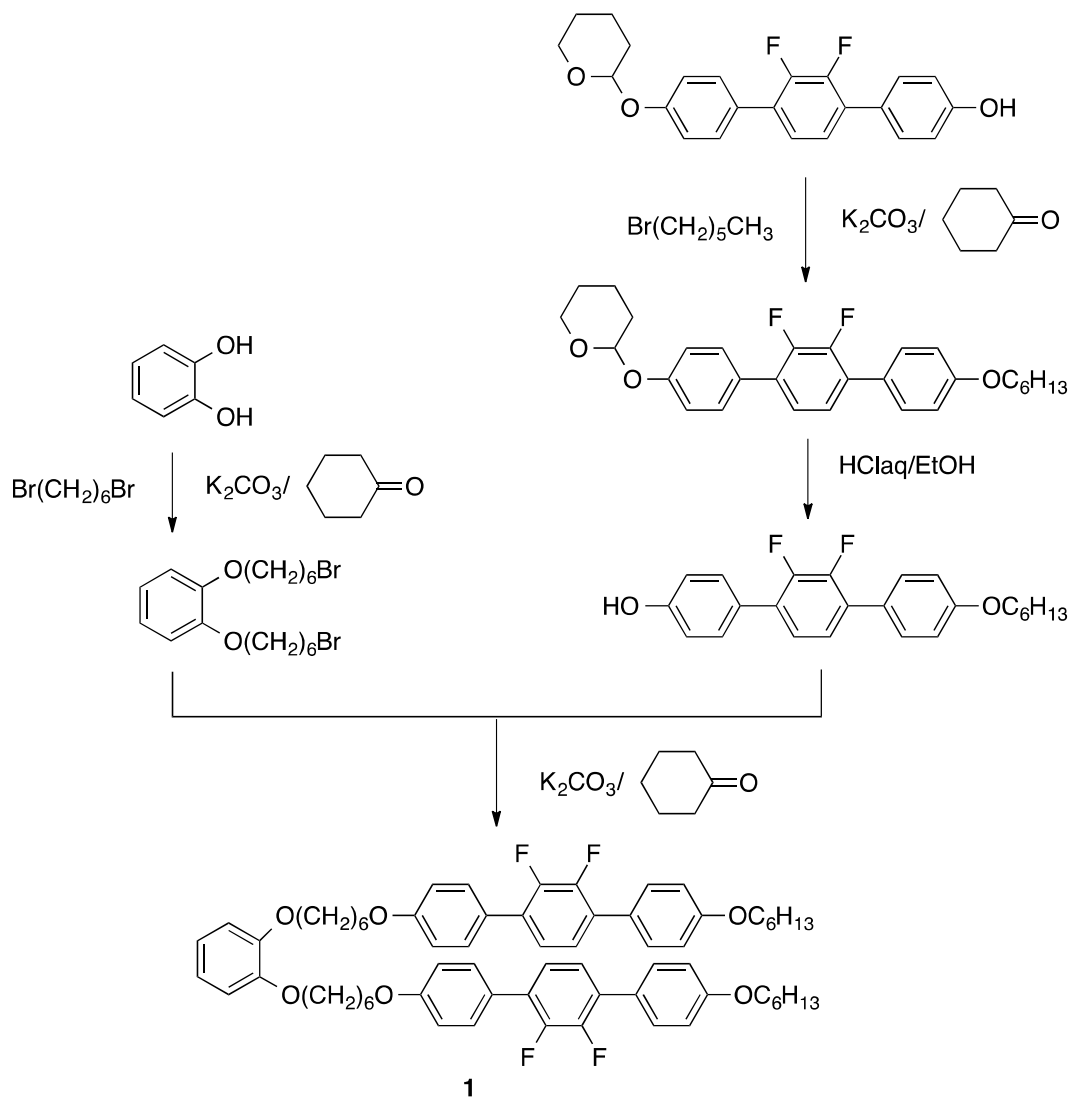
1,4-Bis(4-hexyloxyphenyl)-2,3-difluorobenzene (2). mp 107.9–108.1 °C. ¹H-NMR (500 MHz, CDCl₃, TMS) δ_H/ppm: 7.52 (d, 4H, Ar-H, *J* = 8.6 Hz), 7.18–7.23 (m, 2H, Ar-H), 6.99 (d, 4H, Ar-H, *J* = 8.6 Hz), 4.02 (t, 4H, -OCH₂-, *J* = 6.6 Hz), 1.36–1.82 (m, 16H, aliphatic-H), 0.92(t, 6H, -CH₃, *J* = 7.2 Hz). IR(KBr) ν cm⁻¹: 3434, 1609, 1526, 1458, 1110, 815. Elemental analysis: Found: C% 77.10; H% 7.67, Calc. for C₃₀H₃₆O₂F₂: C% 77.22; H% 7.78

4-[4-(6-Hydroxyhexyloxy)phenyl]-1-(4-hexyloxyphenyl)-2,3-difluorobenzene (3). mp 120.7–121.0 °C. ¹H-NMR (500 MHz, CDCl₃, TMS) δ_H/ppm: 7.52 (d, 4H, Ar-H, *J* = 8.6 Hz), 7.21 (d, 2H, Ar-H, *J* = 4.0 Hz), 6.99 (d, 4H, Ar-H, *J* = 8.6 Hz), 4.02 (t, 4H, -OCH₂-, *J* = 6.3 Hz), 3.68 (q, 2H, -CH₂-OH, *J* = 6.3 Hz), 1.83–1.36 (m, 16H, aliphatic-H), 1.23 (s, 1H, -CH₂-OH), 0.92(t, 3H, -CH₃, *J* = 7.5 Hz). IR(KBr) ν cm⁻¹: 3365, 1609, 1525, 1458, 1091, 813. Elemental Analysis: Found: C% 74.66; H% 7.52, Calc. for C₃₀H₃₆O₃F₂: C% 74.77; H% 7.30.

1,4-Bis[4-(6-hydroxyhexyloxy)phenyl]-2,3-difluorobenzene (4). mp 145.6–145.9 °C. ¹H-NMR (500 MHz, CDCl₃, TMS) δ_H/ppm: 7.52 (d, 4H, Ar-H, *J* = 8.6 Hz), 7.20 (d, 2H, Ar-H, *J* = 2.9 Hz), 6.99 (d, 4H, Ar-H, *J* = 8.6 Hz), 4.02 (t, 4H, -OCH₂-, *J* = 6.3 Hz),

3.66–3.68 (m, 4H, -CH₂-OH), 1.84–1.47 (m, 16H, aliphatic-H), 1.23 (t, 2H, -CH₂-OH, $J = 5.4$ Hz). IR(KBr) ν cm⁻¹: 3429, 1609, 1526, 1459, 1077, 813. Elemental analysis: Found: C% 72.58; H% 7.09, Calc. for C₃₀H₃₆F₂O₄: C% 72.27; H% 7.28.

4-[4-(4-Methylpentylloxy)phenyl]-1-[4-(6-hydroxyhexylloxy)phenyl]-2,3-difluoro-benzene (5). mp 123.6–124.1 °C. ¹H-NMR (500 MHz, CDCl₃, TMS) δ_{H} /ppm: 7.52 (d, 4H, Ar-H, $J = 8.6$ Hz), 7.20–7.21 (m, 2H, Ar-H, $J = 4.0$ Hz), 6.99 (d, 4H, Ar-H, $J = 8.6$ Hz), 4.04–3.98 (m, 4H, -OCH₂-, $J = 6.3$ Hz), 3.70–3.66 (m, 2H, -CH₂-OH, $J = 6.3$ Hz), 1.83–1.37 (m, 16H, aliphatic-H), 1.24 (t, 1H, -CH₂-OH, $J = 5.2$ Hz), 0.94 (d, 6H, -CH₃, $J = 6.3$ Hz). IR(KBr) ν cm⁻¹: 3422, 1609, 1526, 1462, 1078, 812. Elemental analysis: Found: C% 74.59; H% 7.66, Calc. for C₃₀H₃₆O₃F₂: C% 74.66; H% 7.52.

Scheme 1 Synthesis of compound **1**.

Liquid-crystalline and physical properties

The initial phase assignments and corresponding transition temperatures for the products were determined using thermal optical microscopy with a polarizing microscope (POL, Optiphoto; Nikon Corp.) equipped with a microfurnace (FP82; Mettler Inst. Corp.) and a control unit (FP80). Temperatures and enthalpies of transitions were investigated using differential scanning calorimetry (DSC, DSC 6200 calorimeter; Seiko Corp.).

The XRD patterns of the sample during cooling processes were obtained using a

real-time X-ray diffractometer (D8 Discover; Bruker AXS GmbH) or MicroMax-007HF (Rigaku Corp.). A sample was put on a convex lens, which was then placed in a custom-made temperature stabilized holder (stability within ± 1 °C). The phase transition of the sample under the X-ray beam was monitored by observing the texture simultaneously using polarised light microscopy with a charge-coupled device (CCD) camera. The X-ray apparatus was equipped with a cross-coupled Göbel mirror on a platform system with a two-dimensional position-sensitive proportional counter (PSPC) detector (HI-Star; Bruker AXS GmbH). Then X-rays were generated at 45 kV and 20 mA; a parallel Cu K α X-ray beam was used to irradiate the sample.

The correlation length along the layer normal (ξ) was determined using the Ornstein–Zernicke expression as follows. First the X-ray profile as a function of 2θ is converted to a scattering function of q according to:

$$q = (4\pi/\lambda)\sin \theta. \quad (1)$$

By fitting the X-ray profiles using the following Lorentzian equation, the correlation length ξ is determined.

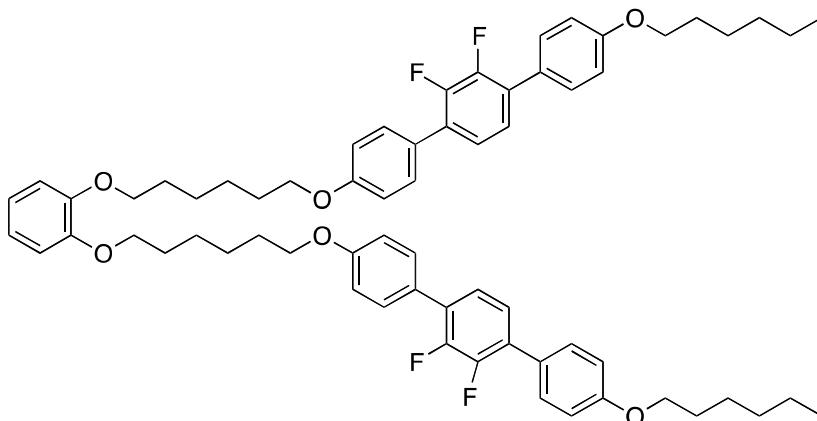
$$I(q) = \frac{I_0}{1 + (q - q_0)^2\xi^2} + \text{background} \quad (2)$$

Therein, I_0 and q_0 respectively signify the peak height and the peak position of q .

Results and discussion

U-shaped system

The first approach for stabilizing an Ncyb phase is inducing lateral correlation in each layer using a U-shaped system. The molecular structure and the phase transition temperatures determined using POM and DSC are presented in Fig. 2. The compound exhibited nematic and smectic C phases. Although the N–SmC transition did not accompany the enthalpy change, a typical fan texture was observed in the SmC phase.



1: Cry 131.6 (73) [SmC 138.2 (^a)] N 196.0 (1.76) Iso

Fig. 2 Molecular structure, transition temperatures (°C) and enthalpies (kJ mol⁻¹, in parentheses) of transition for compound **1**. ^aToo small to be detected.

Fig. 3 shows X-ray diffraction patterns in the small angle region of compound **1** in the N and SmC phases. Alignment was performed by slow cooling of a small drop of a sample on a glass plate. On cooling the sample, a diffuse scattering appeared beside the meridian in the nematic phase (Fig. 3(b)), indicating that molecules are organized in a cybotactic cluster that has an SmC-like skewed structure. However the molecular alignment was insufficient, we cannot determine a detailed structure of the cluster based on the diffraction pattern. The scattering became sharp in the SmC phase (Fig. 3(c)).

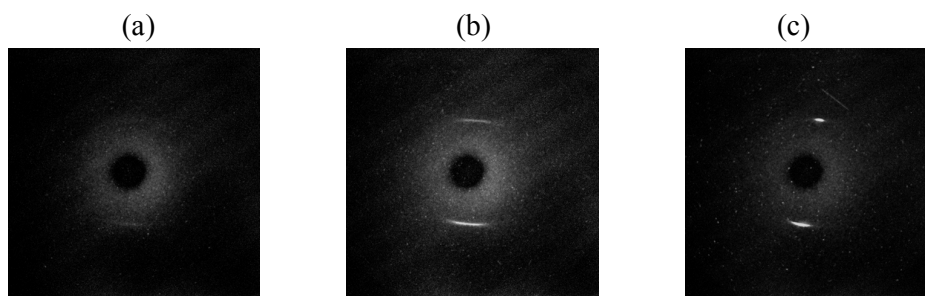


Fig. 3 X-ray diffraction patterns in the small angle region of compound **1**: (a) N phase at $T-T_{NC} = +24.2$ K; (b) N phase at $T-T_{NC} = +4.2$ K; (c) SmC phase at $T-T_{NC} = -0.8$ K.

Fig. 4 shows the X-ray diffraction profile of compound **1** in the N and SmC phases. Fig. 5(a) exhibits the temperature dependence of the layer spacing of compound **1**. The Ncyb

phase appeared at $T-T_{\text{NC}} = +20$ K. The molecular length of compound **1** using MOPAC is estimated as 33 Å. Both Ncyb and SmC phases have a monolayer structure. The layer spacing decreases continuously in the Ncyb phase and the SmC phase with decreasing temperature, indicating that the Ncyb phase has an SmC-like layer structure. Fig. 5(b) shows temperature dependence of the correlation length of compound **1** in the Ncyb and SmC phases. The correlation length increases discontinuously at the Ncyb–SmC transition.

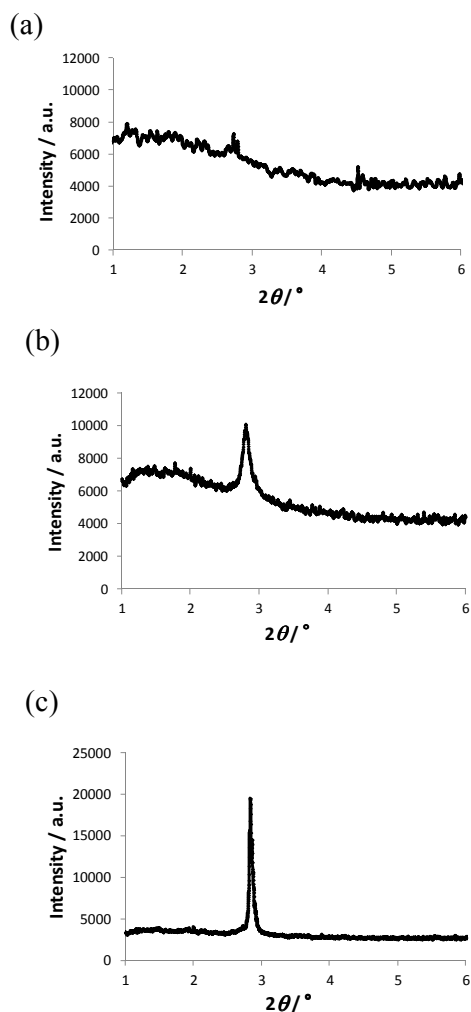


Fig. 4 X-ray diffraction profiles in the small angle region of compound **1**: (a) N phase at $T-T_{\text{NC}} = +24.2$ K; (b) N phase at $T-T_{\text{NC}} = +4.2$ K; (c) SmC phase at $T-T_{\text{NC}} = -0.8$ K.

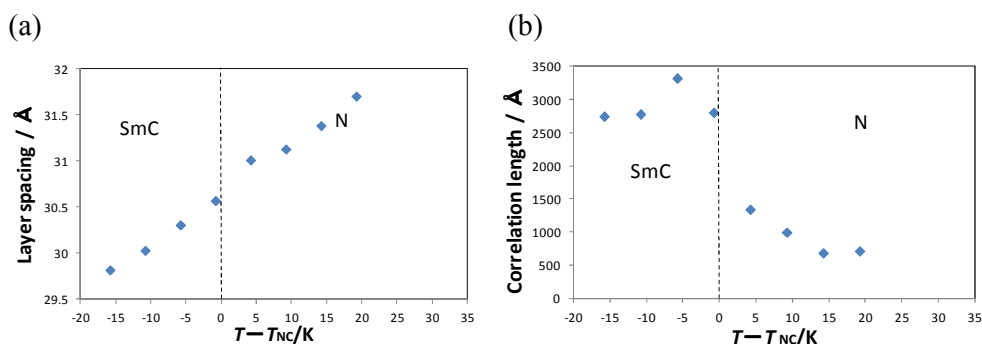
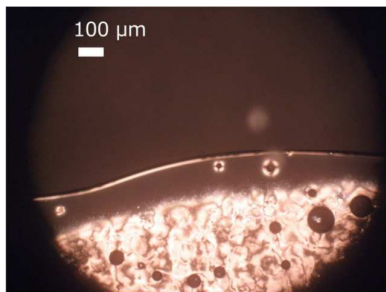


Fig. 5 Temperature dependence of (a) layer spacing and that of (b) correlation length of compound **1** in the N and SmC phases.

Fig. 6 shows optical textures of compound **1** in the N phase at $T - T_{NC} = +34.1$ K and the Ncyb phase $T - T_{NC} = +12.1$ K. Both textures have homeotropic alignment regions and planar alignment regions. In the Ncyb phase, the homeotropic region shows a completely dark texture. Biaxiality was not detected in the Ncyb phase. Considering XRD and POM studies, the director is perpendicular with respect to the glass plate and the layer normal is tilted with respect to the glass plate. The Ncyb phase is thought to have a skewed structure (Fig. 1 left). The Ncyb–SmC transition shows discontinuous increase, however, it did not accompany enthalpy change. The interlayer translational diffusion constant is thought to decrease continuously in the Ncyb and SmC phases, as observed for the Ncyb–SmA transition of the *n*-hexyl derivative.⁴¹ On the other hand, the previously reported U-shaped system possessing two phenylpyrimidine units exhibited a first order Ncyb–SmC transition.³⁶ The intermolecular interaction due to the C–F bond of compound **1** contributes to stabilize the layer ordering in the N phase.

(a) N phase



(b) Ncyb phase

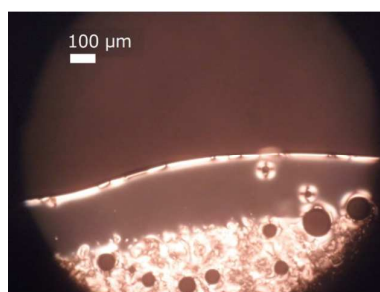
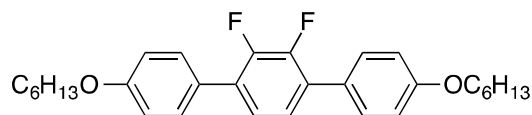


Fig. 6 Optical textures of compound **1** in (a) the N phase at $T - T_{NC} = +34.1$ K and (b) the Ncyb phase at $T - T_{NC} = +12.1$ K.

We observed phase transition behaviour of its monomeric compound (Fig. 7). The compound has the same phase sequence as compound **1**. However, it showed no diffraction pattern in the small angle region corresponding to the layer structure in the N phase.



2: Cry 108.6 (16) SmC 112.5 (0.44) N 172.5 (0.82) Iso

Fig. 7 Molecular structure, transition temperatures ($^{\circ}\text{C}$) and enthalpies (kJ mol^{-1} , in parentheses) of transition for monomeric compound **2**.

U-shaped compound **1** has the following characteristics: (a) strong correlation of rotation around the long axis of each mesogenic group and (b) lateral intermolecular interaction because of the C–F bond. C-13 NMR studies of a smectic liquid crystal suggest that cooperative motion for the mesogenic parts contributes to the orientational order of the molecules in each layer.⁴² Therefore, the U-shaped system enhances lateral interactions producing smectic-like positional order and induces a layer structure with a short correlation length in the N phase. The smectic-like structures can coexist with nematic molecules as presented in Fig. 8.

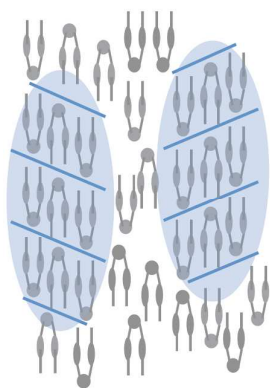


Fig. 8 Model for the Ncyb phase of compound **1**.

Hydrogen-bonding system

The second approach for stabilizing Ncyb phase is regulation of interlayer interaction. Our previous studies on the *n*-hexyl derivative exhibiting an Ncyb phase revealed that the generation of cybotactic clusters affects not only the static structure but also the dynamics in the N phase.⁴¹ To investigate the effects of interlayer interaction on formation of a Ncyb phase, we prepared its derivatives with different terminal groups and observed their phase transition behaviour. Molecular structures and phase transition properties of the compounds are shown in Fig. 9. Molecular lengths of compounds **1–3** using MOPAC are estimated as 29 Å for **3**, 27 Å for **4**, and 27 Å for **5**.

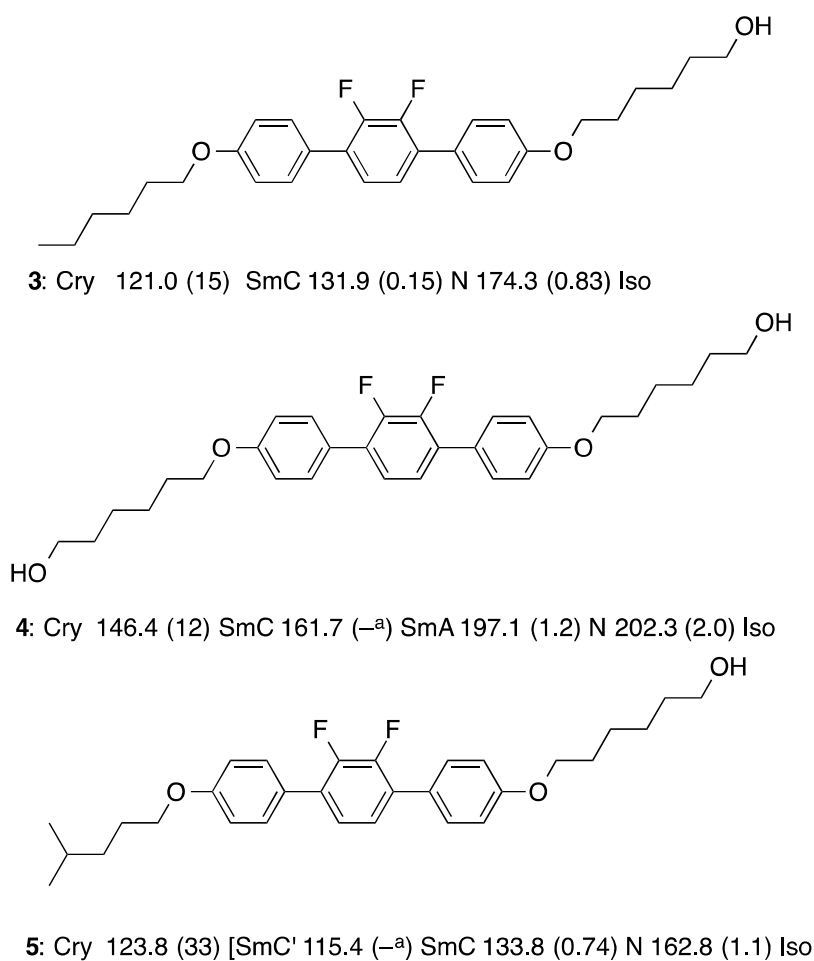


Fig. 9 Molecular structures, transition temperatures (°C) and enthalpies (kJ mol⁻¹, in parentheses) of transition for compounds **3**, **4**, and **5**. ^aToo small to be detected.

XRD profiles of compound **3** in the N and SmC phases are presented in Fig. 10.

Diffraction peak was observed in the N phase (Fig. 10(a)), revealing that compound **3** exhibits an Ncyb phase. The correlation length increased discontinuously at the Ncyb–SmC transition as same as compound **1**. Fig. 11 shows the temperature dependence of (a) layer spacing and that of (b) correlation length of compound **3** in the N and SmC phases. The X-ray diffraction peak appears over 25 K above the N–SmC transition point of compound **3**. Both Ncyb and SmC phases of compound **3** were found to have a monolayer structure. The layer spacing increases and then decreases slightly as decreasing temperature in the Ncyb phase. It shows a discontinuous decrease at the Ncyb–SmC transition, as observed for a typical SmA–SmC transition. The temperature dependence of layer spacing for compound **3** in the Ncyb phase differs from that for compound **1**. There might be difference between them in terms of the layer structure. The optical texture of a homeotropic alignment sample of compound **3** appears to be completely dark. We infer that the Ncyb phase of compound **3** has an SmA-like normal layer structure (Fig. 1 right).

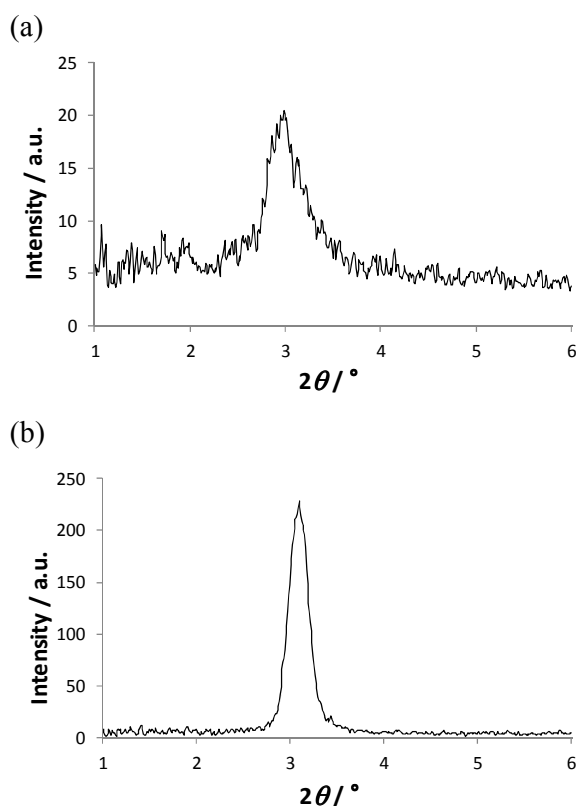


Fig. 10 X-ray diffraction profiles in the small angle region of compound **3**: (a) N phase at $T - T_{\text{NC}} = +13.0$ K; (b) SmC phase at $T - T_{\text{NC}} = -2.0$ K.

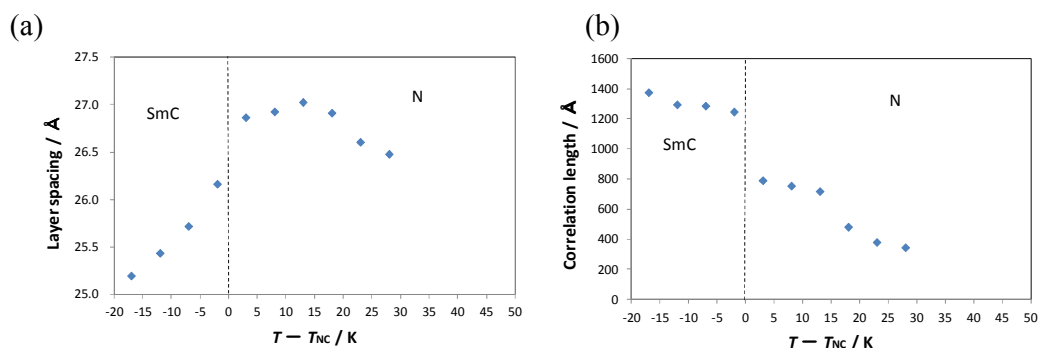


Fig. 11 Temperature dependence of (a) layer spacing and that of (b) correlation length of compound **3** in the N and SmC phases.

Fig. 12 portrays the temperature dependence of the periodicity length of compound **4** possessing two terminal hydroxyl groups in the N and SmA phases. No diffraction peak corresponding to layer spacing was detected in the N phase.

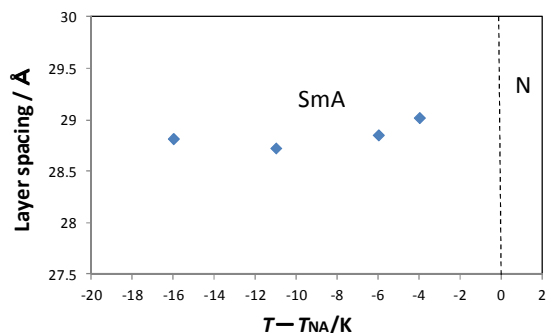


Fig. 12 Temperature dependence of the periodicity length in the N and SmA phases for compound **4**.

Compound **5** was found to exhibit another SmC phase, denoted as SmC' phase. The SmC–SmC' transition did not accompany enthalpy change. Fig. 13 shows a photomicrograph of the sample on the glass in the SmC' phase. The texture of the SmC' phase is similar to that of a modulated bilayer SmC phase observed for the *n*-hexyl derivative.^{38,39}

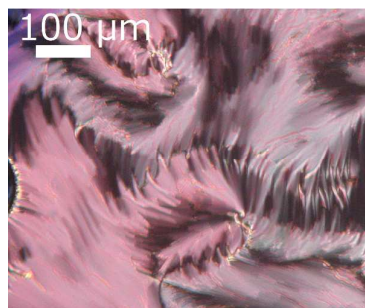
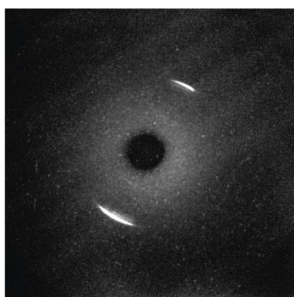


Fig. 13 Optical texture of compound **5** on a glass slide with a cover glass in the SmC' phase at $T-T_{\text{NC}} = -20$ K.

Fig. 14 presents X-ray diffraction patterns in the small angle region of compound **5** in the SmC and SmC' phases. In the SmC phase, scattering corresponding to a layer spacing of 25 Å was observed. The SmC phase was found to have a monolayer structure. Cooling to the SmC' phase, two diffraction spots at small angle appear symmetrically with respect to the diffraction spot corresponding to the monolayer structure. Such a pattern is observed in a modulated smectic phase.^{43,44} Both POM and XRD studies reveal that the SmC' phase is a modulated bilayer SmC phase possessing an in-plane modulation of molecular arrangement.³⁹ At present we cannot exclude a possibility that the SmC' phase has a bilayer structure observed for the SmC'' phase of the *n*-hexyl derivative.³³ However, no diffraction peak corresponding to layer spacing was detected in the N phase of compound **5**. Fig. 15 shows temperature dependences of the periodicity lengths in the N, SmC, and SmC' phases for compound **5**.

(a) SmC



(b) SmC'

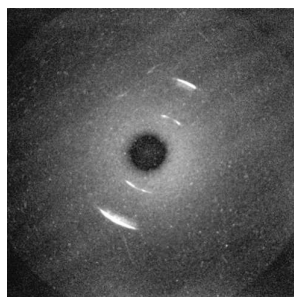


Fig. 14 X-ray diffraction patterns in the small angle region of compound **5**: (a) SmC phase at $T-T_{\text{NC}} = -13.4$ K; (b) SmC' phase at $T-T_{\text{NC}} = -25.4$ K.

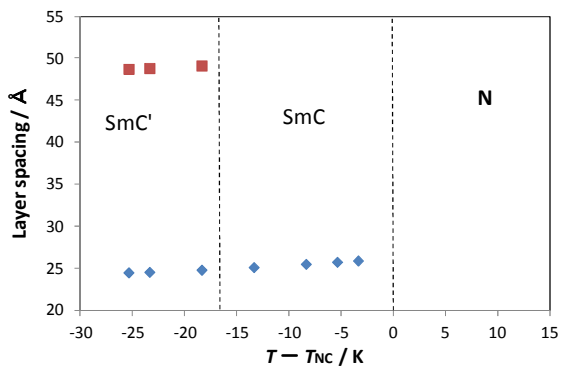


Fig. 15 Temperature dependence of periodicity lengths in the N, SmC, and SmC' phases for compound **5**.

We propose a possible model for appearance of the Ncyb phase of compound **3** as depicted in Fig. 16. Anti-parallel molecular alignment because of micro-segregation prefers a bilayer structure, whereas parallel molecular alignment because of packing entropy prefers a monolayer structure. For a bilayer structure, inter-layer interaction between adjacent alkyl chains is much weaker than intra-layer interaction because of hydrogen bonding, which might destabilize a smectic-like layer structure possessing a long-range periodicity (right hand in Fig. 16). However, in the case of the monolayer structure, it has no difference in inter-layer interaction, which might stabilize a layer structure in the N phase (left hand in Fig. 16). Competition between monolayer and bilayer characters can induce the generation and decomposition of a smectic-like layer structure in the N phase.

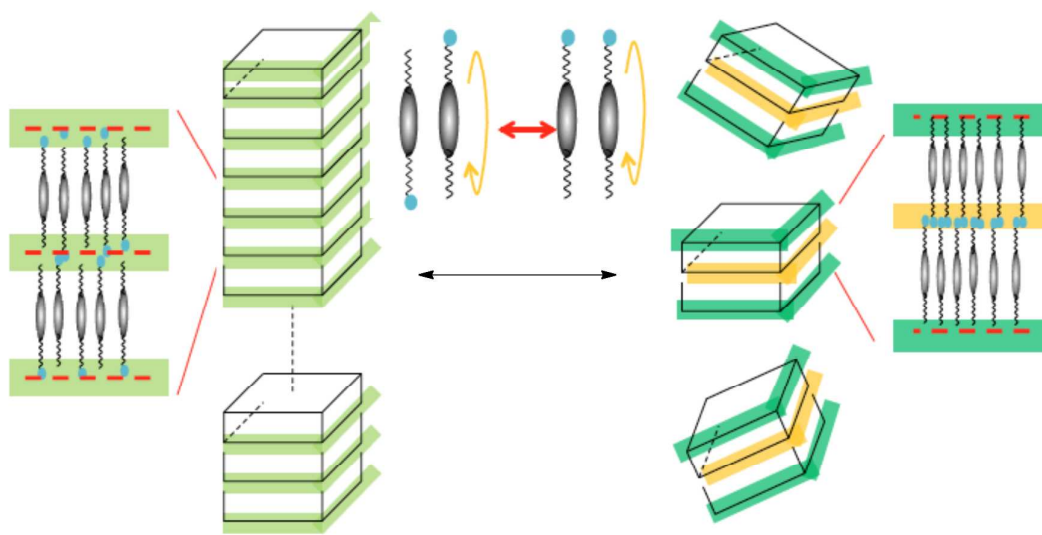


Fig. 16 Possible model for formation of the Ncyb phase of compound 3.

With respect to compound 4 possessing two terminal hydroxyl groups, every inter-layer interaction caused by hydrogen bonding is so strong that the smectic phases are greatly stabilized. Regarding compound 5, the modulated structure was observed in the SmC' phase as observed for the *n*-hexyl derivative possessing an Ncyb phase. However, the N phase of compound 5 has no cybotactic structure. The phase transition behaviour of an anti-clinic smectic liquid crystal possessing a terminal branched group reveals that the inter-layer interaction between adjacent branched chains is stronger than that between linear chains.⁴⁵ The inter-layer interactions between adjacent branched chains for compound 5 might disturb the layer structure decomposition. The smectic phases of compound 5 are stable, and the generation and decomposition of a layer ordering occurs only with difficulty in the N phase.

Conclusions

We propose two molecular designs for a cybotactic nematic phase. The first approach for producing an Ncyb phase is inducing lateral correlation in each layer using a U-shaped system. The U-shaped compound might enhance intra-layer interaction, producing a stable smectic-like layer ordering with a short correlation length in the N phase. The second one is regulation of inter-layer interaction using a hydrogen-bonding system. Competition between monolayer and bilayer characters can induce the

generation and decomposition of a smectic-like layer in the N phase.

Acknowledgement

This work was supported by a Grant-in-Aid for Scientific Research (no. 25107702) on the Innovation Areas: "Fusion Materials" (Area no 22006) from MEXT.

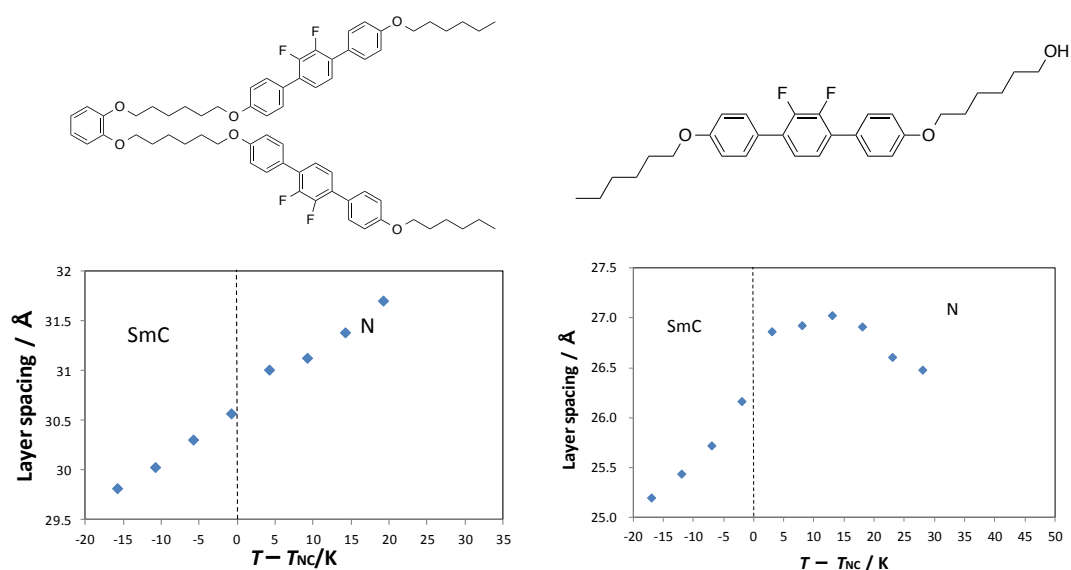
References

1. A. De Vries, *Mol. Cryst. Liq. Cryst.*, 1970, **10**, 319.
2. A. De Vries, *Mol. Cryst. Liq. Cryst.*, 1973, **20**, 119.
3. I. G. Chystyakov and W. M. Chaikowsky, *Mol. Cryst. Liq. Cryst.*, 1969, **7**, 269.
4. A. J. Leadbetter, in *Thermotropic Liquid Crystals. Critical Reports on Applied Chemistry*, ed. G. W. Gray, Wiley, Chichester, 1987, pp. 1-27.
5. M. J. Freiser, *Phys. Rev. Lett.*, 1970, **24**, 1041.
6. R. Berardi, L. Muccioli and C. Zannoni, *J. Chem. Phys.*, 2008, **128**, 024905.
7. F. Hessel and H. Finkelmann, *Polym. Bull.*, 1986, **15**, 349.
8. R. Alben, *Phys. Rev. Lett.*, 1973, **30**, 778.
9. R. Berardi and C. Zannoni, *J. Chem. Phys.*, 2000, **113**, 5971.
10. T. C. Lubensky and L. Radzihovsky, *Phys. Rev. E: Stat., Nonlinear, Soft Matter Phys.*, 2002, **66**, 031704.
11. M. Lehmann, *Liq. Cryst.*, 2011, **38**, 1389 and references cited therein.
12. I. D. Fletcher and G. R. Luckhurst, *Liq. Cryst.*, 1995, **18**, 175.
13. R. W. Date and D. W. Bruce, *J. Am. Chem. Soc.*, 2001, **123**, 10115.
14. P. H. J. Kouwer and G. H. Mehl, *J. Am. Chem. Soc.*, 2003, **125**, 11172.
15. L. A. Madsen, T. J. Dingemans, M. Nakata and E. T. Samulski, *Phys. Rev. Lett.*, 2004, **14**, 145505.
16. B. R. Acharya, A. Primak and S. Kumar, *Phys. Rev. Lett.*, 2004, **14**, 145506.
17. O. Francescangeli and E. T. Samulski, *Soft Matter*, 2010, **6**, 2413.
18. A. G. Vanakaras and D. J. Photions, *J. Chem. Phys.*, 2008, **128**, 154512.
19. C. Tschierske and D. J. Photions, *J. Mater. Chem.*, 2010, **20**, 4283.
20. E. T. Samulski, *Liq. Cryst.*, 2010, **37**, 669.
21. C. Keith, A. Lehmann, U. Baumeister, M. Prehm and C. Tschierske, *Soft Matter*, 2010, **6**, 1704.
22. S. Taushanoff, K. V. Le, J. Williams, R. J. Twieg, B. K. Sadashiva, H. Takezoe and A. Jakli, *J. Mater. Chem.*, 2010, **20**, 5893.

23. H.-C. Jeong, S. Aya, S. Kang, F. Araoka, K. Ishikawa and H. Takezoe, *Liq. Cryst.*, 2013, **40**, 951.
24. S. H. Hong, R. Verduzco, J. C. Williams, R. J. Twieg, E. DiMasi, R. Pindak, A. Jakli, J. T. Gleesona and S. Sprunt, *Soft Matter*, 2010, **6**, 4819.
25. O. Francescangeli, F. Vita, C. Ferrero, T. Dingemans and E. T. Samulski, *Soft Matter*, 2011, **7**, 895.
26. M. Nagaraji, A. Lehmann, M. Prehm, C. Tschierske and J. K. Vij, *J. Mater. Chem.*, 2011, **21**, 17098.
27. G. Shanker, M. Prehm, M. Nagaraji, J. K. Vij and C. Tschierske, *J. Mater. Chem.*, 2011, **21**, 18711.
28. R. A. Reddy, C. Zhu, R. Shao, E. Korblova, T. Gong, Y. Shen, E. Garcia, M. A. Glaser, J. E. MacLennan, D. M. Walba and N. A. Clark, *Science*, 2011, **332**, 72.
29. C. Zhu, R. Shao, R. A. Reddy, D. Chen, Y. Shen, T. Gong, M. A. Glaser, E. Korblova, P. Rudquist, J. E. MacLennan, D. M. Walba and N. A. Clark, *J. Am. Chem. Soc.*, 2012, **134**, 9681.
30. G. Shanker, M. Prehm and C. Tschierske, *Beilstein J. Org. Chem.*, 2012, **8**, 472.
31. G. Shanker, M. Prehm and C. Tschierske, *J. Mater. Chem.*, 2012, **22**, 168.
32. F. Speetjens, J. Lindborg, T. Taucher, N. LaFemina, J. Nguyen, E. T. Samulski, F. Vita, O. Francescangeli and E. Scharrer, *J. Mater. Chem.*, 2012, **22**, 22558.
33. A. Chakraborty, M. K. Das, B. Das, A. Lehmann and C. Tschierske, *Soft Matter*, 2013, **9**, 4273.
34. F. Vita, I. F. Placentino, E. T. Samulski, and O. Francescangeli, *Mol. Cryst. Liq. Cryst.*, 2013, **573**, 46.
35. C. Zannoni, *J. Mater. Chem.*, 2001, **11**, 2637.
36. A. Yoshizawa and A. Yamaguchi, *Chem. Comm.*, 2002, 2060.
37. A. Yoshizawa, *J. Mater. Chem.* 2008, **18**, 2877.
38. A. Yoshizawa, A. Nishizawa, K. Takeuchi, Y. Takanishi and J. Yamamoto, *J. Phys. Chem. B* 2010, **114**, 13304.
39. Y. Kimoto, A. Nishizawa, Y. Takanishi, A. Yoshizawa and J. Yamamoto, submitted to *Phys. Rev. E*.
40. A. Nishizawa, Y. Takanishi, J. Yamamoto and A. Yoshizawa, *Liq. Cryst.*, 2011, **38**, 793.
41. Y. Kimoto, A. Nishizawa, Y. Takanishi, A. Yoshizawa and J. Yamamoto, *J. Phys.*

- Chem. B*, 2013, **117**, 62690.
42. A. Yoshizawa, H. Kikuzaki and M. Fukumasa, *Liq. Cryst.*, 1995, **18**, 351.
 43. G. Sigaud, F. hardouin, M. F. Achard and A. M. Levelut, *J. Physiq.*, 1981, **42**, 1007.
 44. A. M. Levelut, P. S. Pershan, L. B. Sorensen and F. Hardouin, *Phys. Rev. A*, 1981, **24**, 2180.
 45. I. Nishiyama and J. W. Goodby, *J. Mater. Chem.*, 1992, **2**, 1015.

Graphical abstract



We propose two molecular designs for a cybotactic nematic (Ncyb) phase. The U-shaped compound exhibits a skewed Ncyb phase, although the rod-like compound possessing a terminal hydroxyl group shows a normal Ncyb phase.

We propose two molecular designs for a cybotactic nematic (N_{cyb}) phase. The U-shaped compound exhibits a skewed N_{cyb} phase, although the rod-like compound possessing a terminal hydroxyl group shows a normal N_{cyb} phase.